

AD-A252 381



(2)

NASA
Technical Memorandum 105416

AVSCOM
Technical Report 91-C-049

Analysis and Modification of a Single-Mesh Gear Fatigue Rig for Use in Diagnostic Studies

DTIC
ELECTED
JUL 02 1992
S A D

James J. Zakrajsek, Dennis P. Townsend, and Fred B. Oswald
*Lewis Research Center
Cleveland, Ohio*

and

Harry J. Decker
*Propulsion Directorate
U.S. Army Aviation Systems Command
Lewis Research Center
Cleveland, Ohio*

This document has been approved
for public release and sale; its
distribution is unlimited.

May 1992

92-17104



NASA



US ARMY
AVIATION
SYSTEMS COMMAND

**ANALYSIS AND MODIFICATION OF A SINGLE-MESH GEAR FATIGUE RIG
FOR USE IN DIAGNOSTIC STUDIES**

James J. Zakrajsek, Dennis P. Townsend, and Fred B. Oswald
National Aeronautics and Space Administration
Lewis Research Center
Cleveland, Ohio 44135-3191

and

Harry J. Decker
Propulsion Directorate
U.S Army Aviation Systems Command
Lewis Research Center
Cleveland, Ohio 44135-3191

Accession for	
NTIS CRA&I	
DTIC TAB	
Unannounced	
Justification	
By _____	
Distribution /	
Availability	
Dist	Avail. Specia.
A-1	

SUMMARY

A single-mesh gear fatigue rig was analyzed and modified for use in gear mesh diagnostic research. The fatigue rig allowed unwanted vibration to mask the test-gear vibration signal, making it difficult to perform diagnostic studies. Several possible sources and factors contributing to the unwanted components of the vibration signal were investigated. Sensor mounting location was found to have a major effect on the content of the vibration signal. In the presence of unwanted vibration sources, modal amplification made unwanted components strong. A sensor location was found that provided a flatter frequency response. This resulted in a more useful vibration signal. A major rework was performed on the fatigue rig to reduce the influence of the most probable sources of the noise in the vibration signal. The slave gears were machined to reduce weight and increase tooth loading. The housing and the shafts were modified to reduce imbalance, looseness, and misalignment in the rotating components. These changes resulted in an improved vibration signal, with the test-gear mesh frequency now the dominant component in the signal. Also, with the unwanted sources eliminated, the sensor mounting location giving the most robust representation of the test-gear meshing energy was found to be at a point close to the test gears in the load zone of the bearings.

INTRODUCTION

Drive train diagnostics is becoming one of the most significant areas of research in rotorcraft propulsion. The need for a reliable health-monitoring system for the propulsion system can be seen by reviewing some rotorcraft accident statistics. An investigation of serious rotorcraft accidents that were a result of fatigue failures showed that 32 percent were due to engine and transmission components (Astridge, 1989). Also, 60 percent of the serious rotorcraft accidents were found to occur during cruise flight. Civil helicopters need a thirtyfold increase in their safety record to equal that of conventional fixed-wing turbojet aircraft. Practically, this can only be accomplished by the development of a highly reliable, on-line health-monitoring unit. Diagnostic research is required to develop and prove various fault-detection concepts and methodologies. NASA Lewis Research Center has recently initiated a program to use some of its gear fatigue test facilities for diagnostic research while also continuing fatigue research. This paper documents the analysis and modification that was required to convert a single-mesh gear fatigue rig for diagnostic research.

Single-mesh gear fatigue rigs at NASA Lewis have been used for nearly 20 years to supply data on the effects of gear materials, gear surface treatments, and lubrication types and methods on the fatigue strength of aircraft-quality gears. A schematic diagram and cutaway view of the fatigue rig are shown in figure 1. The test rig is a four-square type with power recirculating through the slave gears. Resisting torque is provided by hydraulically actuated load vanes inside one of the slave gears. The motor provides only the power required to overcome frictional forces. Until recently (Zakrajsek, 1989) this rig was exclusively used for fatigue studies, where only the overall root-mean-square vibration level was monitored as an indicator of failure.

The most critical part of any diagnostic monitoring process is the ability to obtain vibration data that accurately represent the dynamics of the component that is being monitored. In a previous study (Zakrajsek, 1989) a major problem was identified in using this fatigue rig for diagnostic studies. The vibration signal from this rig was found to contain a number of frequency components that were unrelated to the test gears. A typical vibration spectrum from the fatigue rig is given in figure 2. This spectrum was a result of time-synchronous averaging of the signal over 100 revolutions. Time-synchronous averaging reduces the components of the vibration signal that are not coincident with the shaft rotational frequency. Even with time averaging the vibration signal is saturated with vibration components at frequencies other than the test-gear meshing frequency and its harmonics. These components mask the test-gear meshing signal. Applying current diagnostic methods (McFadden, 1986, and Stewart, 1977) to this noisy vibration signal results in confusing and erroneous predictions. The unwanted vibration components of this signal, because they are dominant, have the major influence on the results of the diagnostic methods. A way was needed to obtain a "cleaner" vibration signal that accurately reflects only the dynamics of the test gears before meaningful diagnostic research could be performed with this fatigue rig.

In order to improve the vibration signal for diagnostic research, several steps were taken to analyze and modify the single-mesh gear fatigue rig. The first step involved trying to identify possible sources and factors contributing to the problem. Following this, some analysis was performed on an existing rig to determine the effects of sensor mounting location on the vibration signal. Another rig was then physically modified in an effort to reduce the unwanted vibration components in the signal. The two rigs used in this study were identical in both physical construction and dynamic response. The modified rig was then analyzed to determine how the vibration signal changed. The following sections discuss each of these steps in more depth. Some conclusions based on the results of this study are also presented.

PROBLEM SOURCE IDENTIFICATION

In order to reduce the amplitude of undesired vibration frequencies, several possible sources and factors had to be identified. Resident rotor and gear dynamics experts, general information from the literature, and specific rig geometry information were all used to establish a list of the most probable sources and factors that might result in the unwanted noise. Two methods can be used to reduce this noise: Either eliminate the sources of the noise or minimize the transmission to the sensor. In those cases where the sources cannot be eliminated, reducing the transmission to the sensor of the unwanted components may be the only feasible option. The most probable sources and factors are listed here. The first factor listed can be investigated without modification to the rig.

(1) The accelerometer may not be mounted in an optimum location. Two issues affect the optimum location. First, the optimum location should give the strongest representation of the test gears being monitored. In the case of rolling-element bearings a bearing defect in a helicopter tail rotor gearbox was easier to detect when the accelerometer was closest to the bearing and located in the bearing load zone (Hollins, 1988). Because the vibration must be transmitted through the bearings to the case, it is expected that the gear vibration will also be strongest in the bearing load zone. Second, the vibration signal at the optimum location should have the test-gear meshing frequencies as the dominant components.

(2) The slave gears may be too lightly loaded. The slave gears are also spur gears; however, unlike the test gears the slave gears are oversized to ensure that they do not fail during the test. The normal operating load of the rig results in the slave gears being loaded to approximately 10 percent of their design load based on tooth contact stress, and to 8 percent based on tooth bending stress. Lightly loaded spur gears have a tendency for excessive vibration and noise (Rebbechi et al., 1992). The nonlinear nature of gears losing contact during meshing results in a vibration forcing function that is broadband (i.e., a function that requires a wide band of frequency components to characterize the time signal).

(3) Imbalance may exist in the rotating components. The slave gears and the shafts are balanced separately and then assembled. Even though both are balanced separately, an imbalance could exist after the parts are assembled unless the axes of rotation of both parts are exactly concentric. The vibration due to imbalance will be limited to the first several shaft harmonics.

(4) Misalignment may exist in the rotating components. A bent or misaligned shaft can result in a high level of vibration. The vibration due to misalignment usually results in a large number of shaft harmonics in the spectrum.

(5) Mechanical looseness may exist in the rotating components. The fatigue rig has been in operation for nearly 20 years, and many of the rotating parts now fit loosely due to wear. Bearings fit loosely in the housing, and slave gears fit loosely over shafts. Mechanical looseness is generally characterized by normal sinusoidal vibration interrupted by a mechanical limit. The machine response will be nonlinear, exhibiting a time domain signal containing truncation and impulses. This nonlinear nature of the vibration due to mechanical looseness results in a vibration forcing function that, like that of the lightly loaded slave gears, is broadband (Lyon, 1987).

(6) Slave gears are too massive. The slave gears are roughly 5½ times more massive than the test gears. Excessive slave-gear mass can amplify unwanted vibration sources due to misalignment and imbalance.

ANALYSIS OF UNMODIFIED RIG

Before modifying the test rig some analysis was performed on an existing rig to determine what effect sensor location alone has on the vibration signal. Sensor location is the only one of the six sources and factors identified that can be changed without physically modifying the test rig.

For diagnostic studies the optimum sensor location is that point at which the test-gear meshing frequencies dominate the signal and are more prominent than at any other location. As

shown in figure 2, the main problem is obtaining a vibration signal that is not masked by the other components in the signal. It is believed that these unwanted components in the vibration signal are a result of the natural modes of the vibration transfer path, from the gear mesh to the sensor, being excited by the sources identified previously. Those sources that result in a broadband vibration (e.g., mechanical looseness and lightly loaded slave gears) are capable of exciting most natural modes of the transfer path in the frequency range of interest. The range 1 to 10 kHz is defined as the frequency range of interest, as it contains the primary mesh frequency of the test gear (4741 Hz) and its second harmonic. Therefore, it is possible to reduce the effects of the various sources on the vibration signal by locating the sensor at a point where the modal properties of the transfer path have minimal effect on the signal.

In order to determine the optimum sensor mounting location, frequency response measurements were conducted at 18 locations on the test rig, as illustrated in figure 3. An instrumented modal hammer was used to apply an impulse input on the shaft where the test gear mounts, in the direction that the actual meshing forces act on the shaft, as depicted by vector \vec{T} in figure 3. A common practice used in modal analysis is to analyze the spectrum of the input impulse and determine at what frequency the amplitude drops by 20 dB. The impulse sufficiently excites all the frequencies in the structure up to that point. This is commonly referred to as the 20-dB dropoff rule. Using this rule, the applied impulse was found to excite frequencies up to 9 kHz. Frequency response measurements were taken between the common impulse application point (point O) and each of the 18 locations on the test rig. The magnitude of the frequency response function, or the system gain factor, was recorded at each point. The system gain factor is given as

$$|H(f)| = \frac{|Y(f)|}{|X(f)|}$$

where $|Y(f)|$ = output amplitude and $|X(f)|$ = input amplitude.

In order to measure the quality of the frequency response function obtained, the coherence function was calculated for each frequency response function. The coherence function is a measure of the amount of the output signal that is directly related to the input signal at any specific frequency. A coherence value of 1.0 at a certain frequency indicates that the output at that frequency is a direct result of the input signal at that frequency. The measured coherence was at or very close to 1.0 for all frequencies up to approximately 7.5 kHz. Above 7.5 kHz the coherence dropped off rapidly. Figure 4(b) shows an example of the coherence function obtained for the frequency response measurement of figure 4(a). Thus, the frequency response functions obtained were considered only up to 7.5 kHz, because of the uncertainty of the measurement beyond that point.

Frequency response results are given in figures 4 and 5 for sensor mounting locations 6, 10, 3, and 16, respectively. Of all the locations examined, locations 6 and 10 were found to exhibit the flattest frequency response functions. Locations 6 and 10 are probably coincident with nodes of the housing. Location 3 is the traditional accelerometer mounting point and was used in the previous study (Zakrajsek, 1989). As shown in figure 5(b), location 3 appeared to be more modally active than locations 6 and 10. Location 16 represented the optimum point with respect to previous studies (Hollins, 1986). This position was on the bearing end plate at one of the closest points to the test-gear mesh. As shown in figure 5(c), location 16 was found to be one of the most modally active of the 18 positions analyzed. Other locations on the bearing end

plate that are just as close to the test gears (15, 17, and 18) exhibited nearly identical frequency response results as that found at location 16. The advantage of location 16 over the other locations is its close proximity to the center of the bearing load zone (within 13°). Owing to geometric considerations the center of the bearing load zone is approximately 21° clockwise from the line of action of the test gears. On the basis of transfer function measurements, locations 6 and 10 were the points found most likely to reduce broadband noise source amplification in the vibration signal.

In order to verify the transfer function study, a new set of test gears was installed in the rig and the vibration signal was measured at the various sensor locations. Again, the signal was time-synchronously averaged to remove all vibration components that were not coincident with the shaft rotation. Figure 6 gives the vibration spectrum plots for accelerometer locations 6, 10, 3, and 16. Locations 6 and 10 gave the cleanest vibration signal, with location 10 being the best of the two. The primary meshing frequency of the test gears and their first-order sidebands dominated the vibration signal measured at location 10. In contrast to the relatively clean spectrum at location 10, the spectra at locations 3 and 16 contained a number of frequency components that were not related to the test gears. Many of these unwanted frequency components were stronger than the test-gear meshing frequencies and therefore dominated the vibration signal.

Of particular concern is the large vibration component that was present in the spectra at locations 3 and 16, which was extremely close to a 3200-Hz rig vibration mode. This 3200-Hz mode was dominant in the frequency response measurements at both locations 3 and 16 (figs. 5(b) and (c)). To a lesser degree the 3200-Hz mode was also represented in the frequency response measurement at location 10 (fig. 5(a)). However, only a minor component near 3200 Hz can be seen in the spectrum at location 10 (fig. 6(b)) because the unwanted vibration was not significantly amplified by the modal response. Location 10 is also further from the unwanted sources. Sensor location was found to have a large impact on the components of the vibration signal, with the least modally active point giving the best results in the presence of unwanted vibration sources.

MODIFICATION OF FATIGUE RIG

The fatigue rig was modified to reduce the most probable sources and factors contributing to the unwanted components of the vibration signal. Most of the rework was focused on restoring the fatigue rig to its original design specifications. As stated earlier, the fatigue rig has been in operation for nearly 20 years, resulting in some wear and looseness in the rotating components. In order to reduce looseness and misalignment, the housing was reworked by adding material and remachining the bearing mounting holes. The slave gears were mated with carefully chosen shafts to produce a slight interference fit for the nonactuating gear, as defined in figure 1, and a line fit (zero clearance and zero interference) for the actuating gear. The slave gears were machined to reduce mass and to increase tooth mesh loads. The weight of the slave gear was reduced by 54 percent for the nonactuating and 37 percent for the actuating gear. The tooth face widths for both slave gears were reduced by 50 percent. This reduction in face width resulted in tooth contact stress being increased from 10 percent to 20 percent of the design value. Tooth bending stress was increased from 8 percent to 16 percent of the design stress. The slave gears were balanced after they were machined and then rebalanced after they were mounted on the shafts. This reduced the amount of imbalance in the rotating components.

Figure 7 shows results of the frequency response measurements on the modified rig for locations 10, 3, and 16. Comparing this figure with figure 5 illustrates similar modal characteristics for the modified rig and the existing rig. Location 10 exhibited a relatively flat frequency response function on both rigs. Only two major differences can be seen. At all locations the 1.1-kHz mode on the existing rig shifted to 2.2 kHz on the reworked rig, and at location 16 the large 7.3-kHz mode on the existing rig was absent on the reworked rig. The shift in the lower mode from 1.1 to 2.2 kHz can be explained by the large amount of mass removed from the slave gears on the modified rig.

RESULTS OF RIG MODIFICATION

In order to determine the results of the rig modification, a new set of test gears was run on both the existing rig and the reworked rig. First, the gears were run on the existing rig for a short time while vibration measurements were made at a variety of locations on the rig. The same set of new test gears was then installed and run on the reworked rig, with vibration signals recorded at identical locations. The vibration spectra from the existing rig were compared with those from the modified rig with the same test-gear set for locations 10, 3, and 16, respectively (see figs. 8, 9, and 10). As shown in these figures there was a definite improvement in the spectrum of the vibration signal with the modified rig. At all locations the amplitude of unwanted vibration components near the test-gear meshing frequency was reduced in the reworked rig. The strong components near 3200 Hz at locations 3 and 16 on the existing rig were reduced to negligible values on the reworked rig. The test-gear meshing frequency was more prominent at all locations on the reworked rig as compared with the same locations on the existing rig. These results strongly support the conclusion that the sources of the unwanted vibration were greatly reduced, if not eliminated, as a result of the rework.

One adverse result of the rework was the increase in amplitude at the slave-gear meshing frequency at locations 10 and 3 on the reworked rig. Unfortunately, even though the spectrum was much cleaner and the test-gear meshing frequency was more prominent at locations 10 and 3 on the reworked rig, the slave-gear meshing frequency strength had increased to the point where it was now the dominant component in the vibration signal. It is suspected that the tooth deflection resulting from increasing the slave-gear tooth loading by a factor of 2 caused the initial tooth contact to happen prematurely. Adding some form of tip relief to the presently unmodified slave-gear tooth profile should correct this problem (Lin et al., 1989).

Another problem associated with the current rig was observed while comparing results with the modified rig. Two different sets of new test gears were used to produce the spectra illustrated in figures 6(b) and 8(a) for location 10 on the existing rig. Although two different sets of gears were used, both spectra show the same pattern of lower amplitude for the test-gear primary meshing frequency as compared with the corresponding first-order sidebands. This pattern was not present at location 10 on the reworked rig even though the same gear set was used. In fact, as shown in figure 8, no sidebands were detectable on the reworked rig. Strong first-order sidebands are usually an indication of eccentricity. The problem was found to be a badly worn shaft on the existing rig, with a 0.003-in. clearance between the shaft and the test gear where a line fit is specified. The additional clearance provided by the worn shaft caused eccentric mounting of the gear. The sidebands are a result of the once-per-revolution eccentricity being carried through the primary test-gear meshing frequency.

When extraneous vibration sources are eliminated, the optimum mounting location is that point closest to the gear mesh being monitored in the load zone of the bearing. Figure 10(b) illustrates that when the extraneous vibration sources were removed, location 16 (the closest to the test-gear mesh and in the bearing load zone) gave the strongest representation of the test-gear meshing energy. Figure 10(a) also shows that in the presence of extraneous vibration sources, location 16 was one of the worst locations. If the sources of the noise in the vibration signal could not be eliminated or reduced, location 10 would be the optimum sensor position. Even though the test-gear meshing frequency was not as robust at location 10, the relatively flat frequency response of the transmission path at location 10 served to reduce the influence of the unwanted noise sources to the point where the frequency components of the test-gear mesh dominated the vibration signal.

CONCLUSIONS

A single-mesh gear fatigue rig was analyzed and modified to improve the vibration signal for use in diagnostic studies. Poor accelerometer placement, mechanical looseness, imbalance, and oversized and underloaded slave gears caused the test-gear vibration components to be completely masked by other frequency components. The modifications reduced the unwanted vibration and resulted in a vibration signal that is useful for diagnostic studies. Some significant conclusions of this study are listed here:

- (1) Sensor location has a major effect on the strength of unwanted components in a vibration signal. A location free from resonant amplification of the unwanted vibration components is desirable. If there is no problem with unwanted vibration, the optimum sensor location will likely be near a gear support bearing and in the direction of bearing loading.
- (2) By minimizing imbalance, misalignment, and looseness in rotating parts, unwanted components in the vibration signal can be reduced to negligible levels. Mechanical looseness is especially destructive to a clean vibration signal. The nonlinear nature of the vibration due to mechanical looseness results in a broadband excitation.
- (3) Increasing the tooth load on the slave gears, which have unmodified involute tooth profiles, results in an increase in slave-gear mesh vibration instead of the reduction that is desired.

REFERENCES

- Astridge, D.G., 1989, Helicopter Transmissions - Design for Safety and Reliability. Inst. Mech. Eng. Proc., vol. 203, no. G2, pp. 123-138.
- Hollins, M.L., 1988, The Effects of Vibration Sensor Location in Detecting Gear and Bearing Defects. Deflection, Diagnosis, and Prognosis of Rotating Machinery to Improve Reliability, Maintainability, and Readiness Through the Application of New and Innovative Techniques, T.R. Shives and L.J. Mertaugh, eds., Cambridge University Press, Cambridge, MA, pp. 49-58.
- Lin, H.H., Oswald, F.B., and Townsend, D.P., 1989, Profile Modification to Minimize Spur Gear Dynamic Loading. 1989 International Power Transmission and Gearing Conference, 5th, ASME, Vol. 1, pp. 455-465.

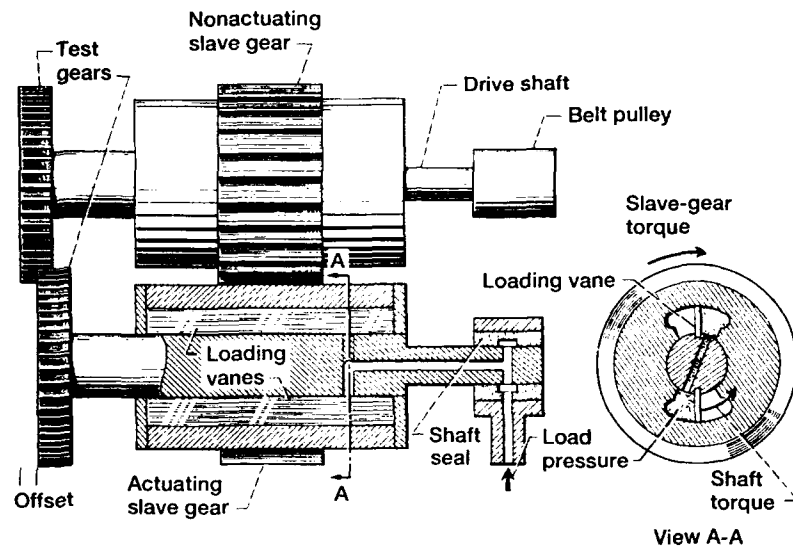
Lyon, R.H., 1987, Machinery Noise and Diagnostics. Butterworth Publishing, Boston.

McFadden, P.D., 1986, Detecting Fatigue Cracks in Gears by Amplitude and Phase Demodulation of the Meshing Vibration. *J. Vib. Acoust. Stress Reliab. Design*, vol. 108, no. 2, Apr. pp. 165-170.

Rebbechi, B.R., et al., 1992, A Comparison Between Theoretical Prediction and Experimental Measurement of the Dynamic Behaviour of Spur Gears. Prepared for the ASME 6th International Power Transmission and Gearing Conference, September 13-16, 1992, Phoenix, AZ.

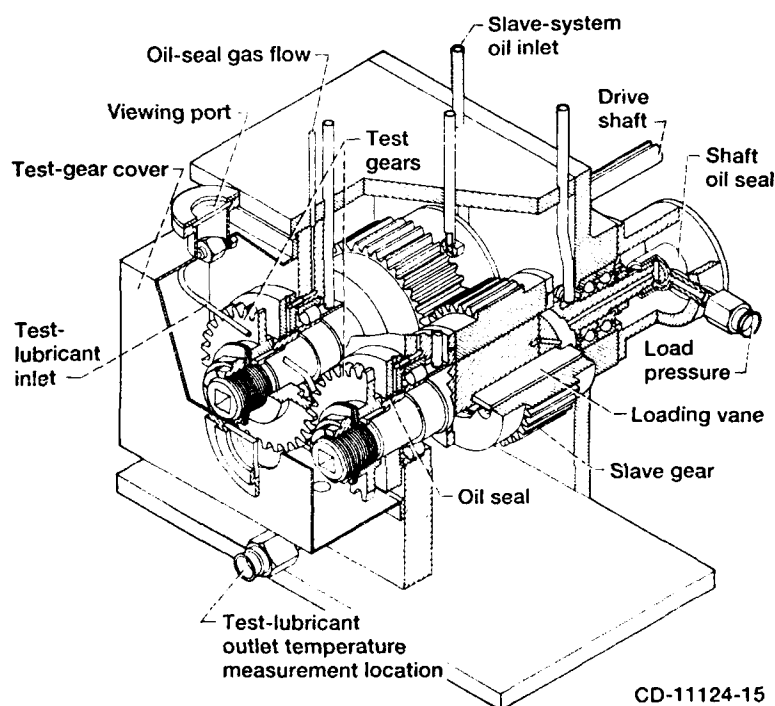
Stewart, R.M., 1977, Some Useful Data Analysis Techniques for Gearbox Diagnostics. Machine Health Monitoring Group, Institute of Sound and Vibration Research, University of Southampton, Report MHM/R/10/77, July.

Zakrajsek, J.J., 1989, An Investigation of Gear Mesh Failure Prediction Techniques. NASA TM-102340.



CD-11421-15

(a) Schematic diagram.



CD-11124-15

(b) Cutaway view.

Figure 1.—Gear fatigue test apparatus.

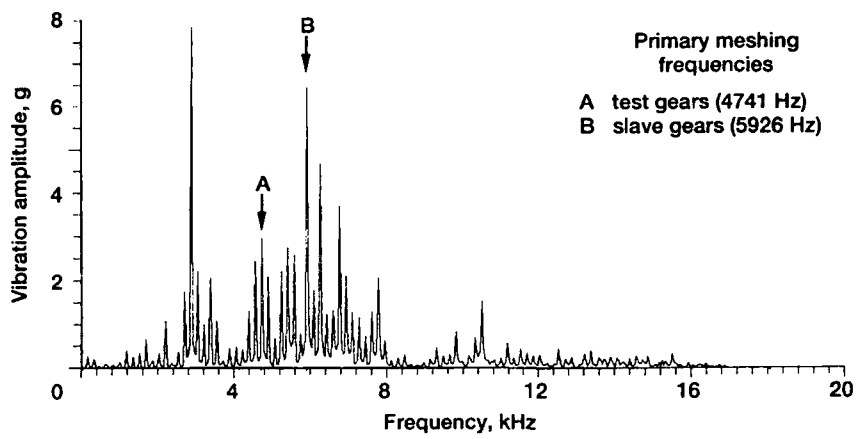


Figure 2.—Typical vibration spectrum from existing single-mesh gear fatigue rig.

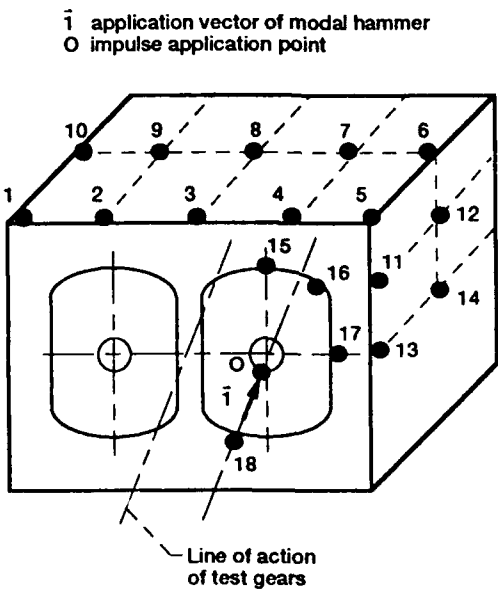
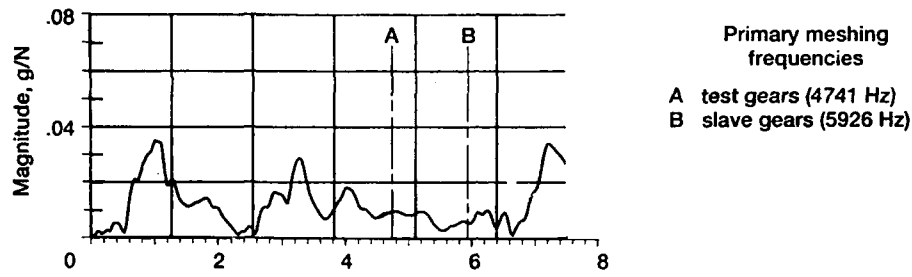
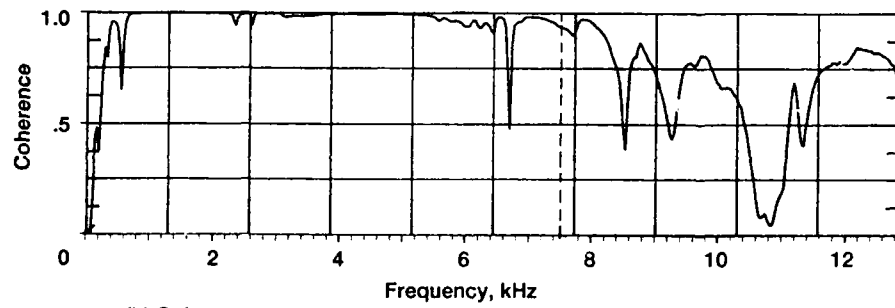


Figure 3.—Sensor mounting locations on fatigue rig.



(a) Magnitude plot of frequency response function on existing rig.



(b) Coherence function for frequency response measurement of figure 4(a).

Figure 4.—Magnitude plot of frequency response function and its coherence function for location 6.

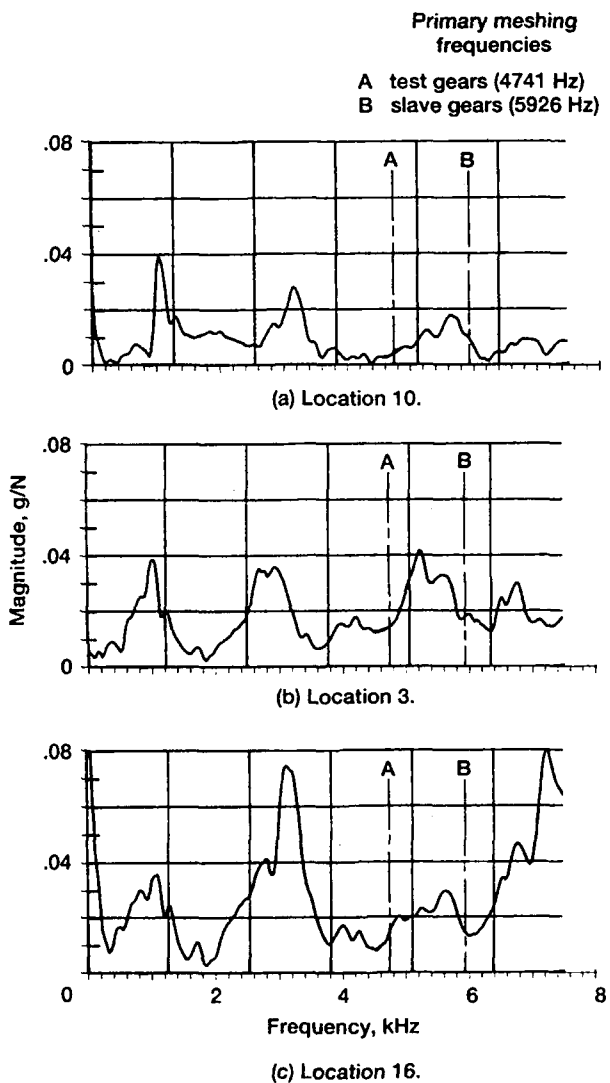


Figure 5.—Magnitude plots of frequency response function for locations 10, 3, and 16 on existing rig.

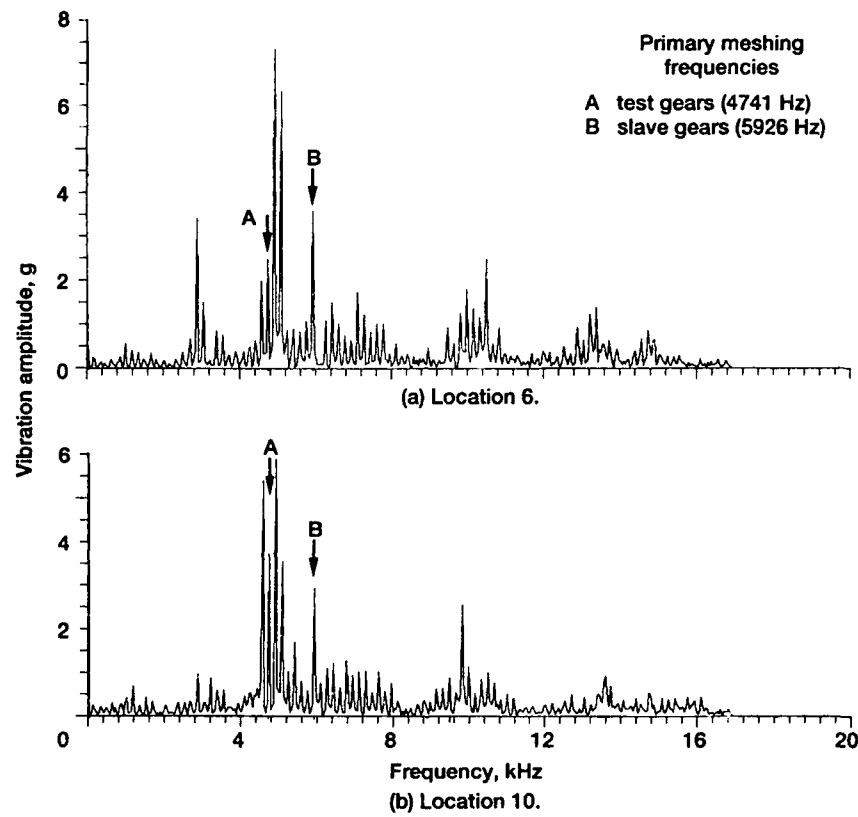


Figure 6.—Vibration spectrum plot for sensor mounting locations 6, 10, 3, and 16 on existing rig.

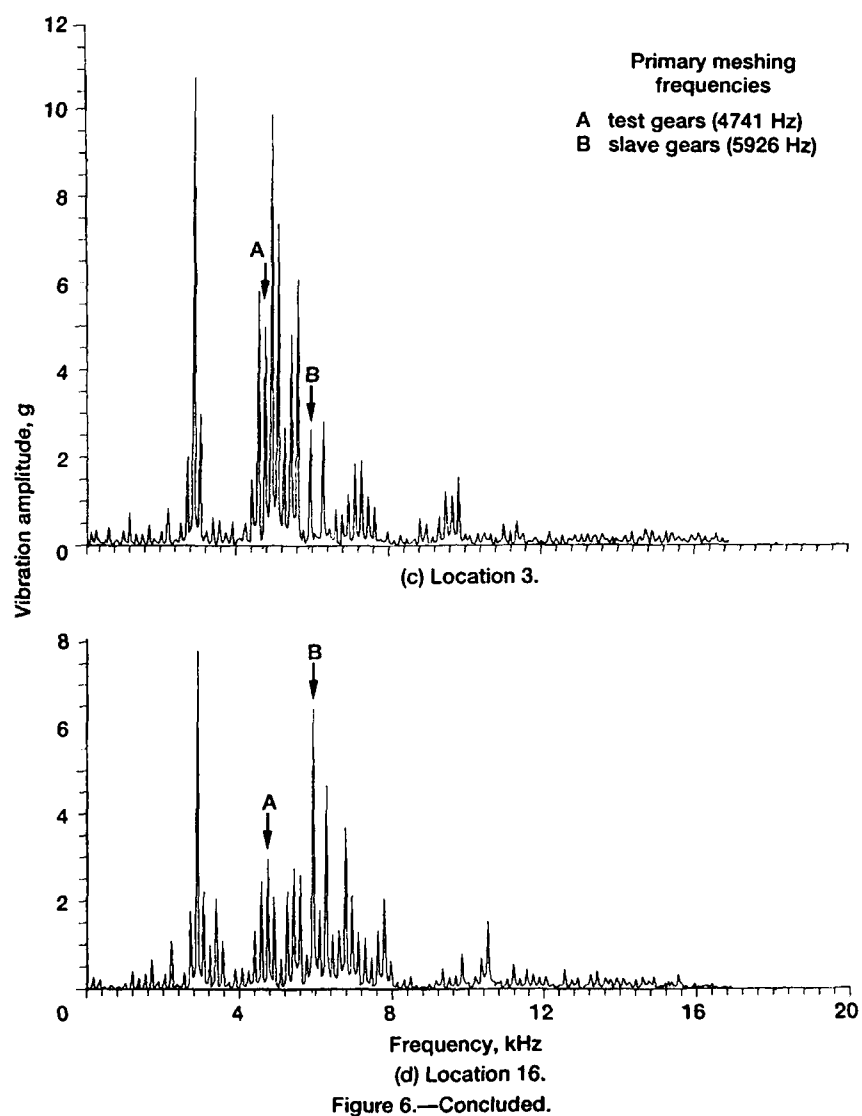


Figure 6.—Concluded.

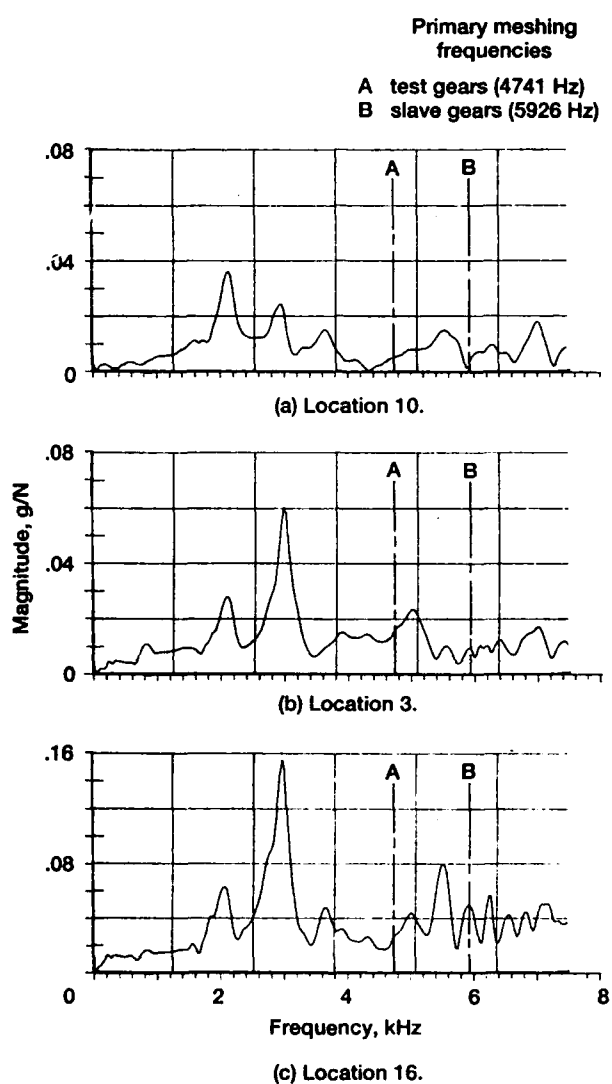


Figure 7.—Magnitude plots of frequency response function for locations 10, 3, and 16 on reworked rig.

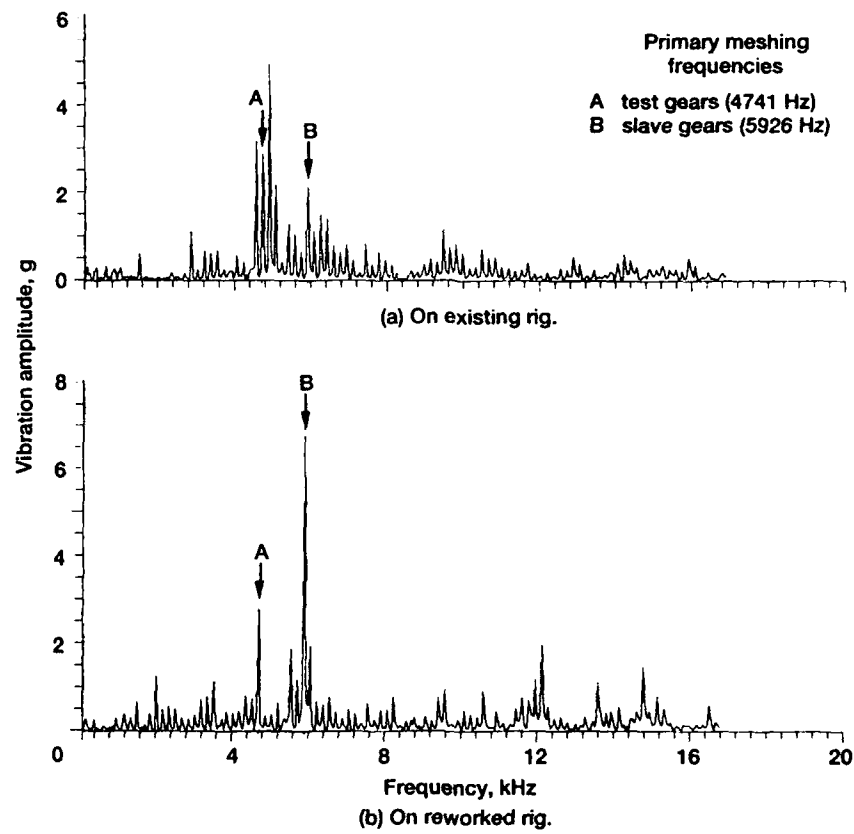


Figure 8.—Vibration spectrum plot of new test gear set with sensor at mounting location 10.

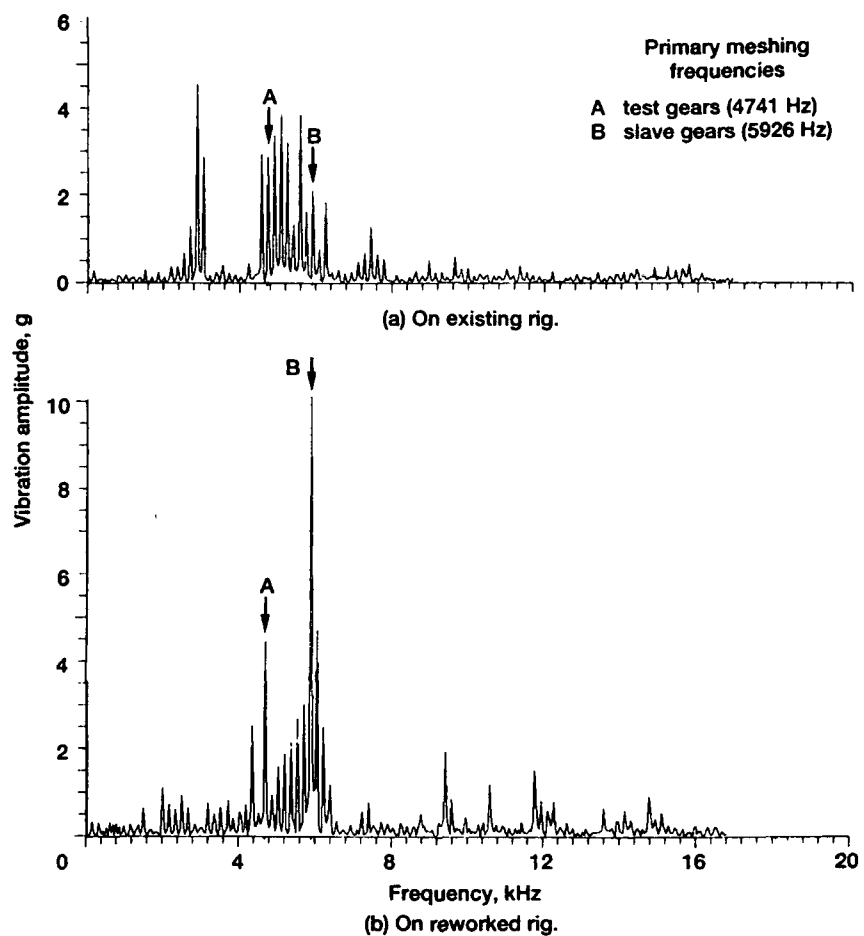


Figure 9.—Vibration spectrum plot of new test gear set with sensor at mounting location 3.

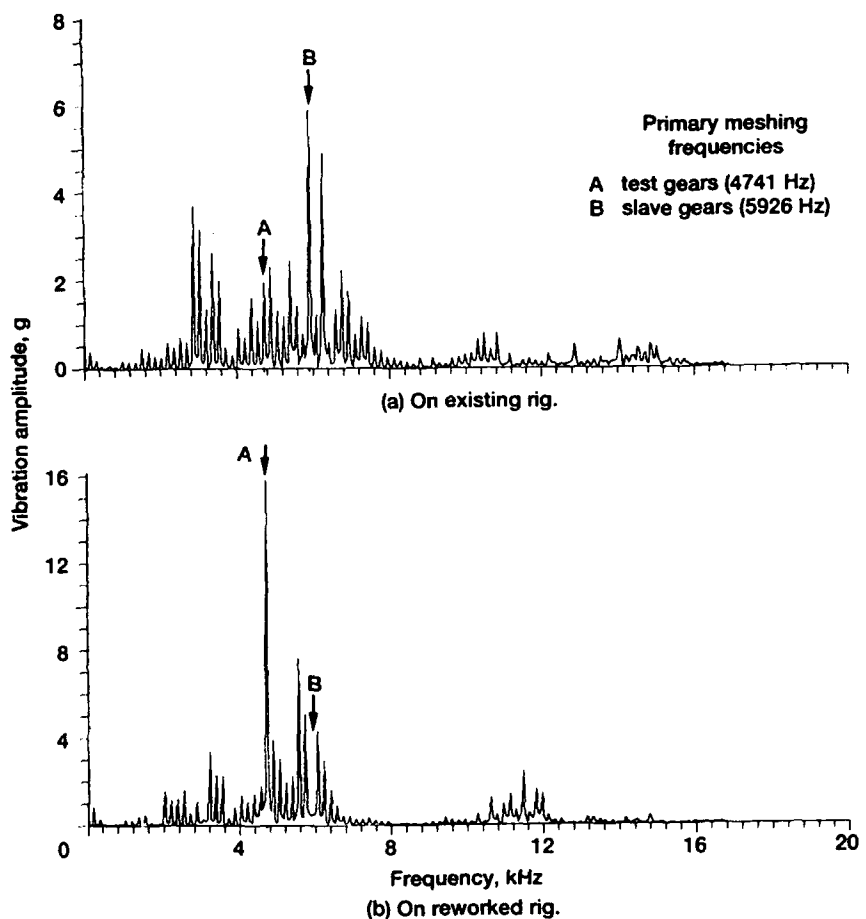


Figure 10.—Vibration spectrum plot of new test gear set with sensor at mounting location 16.

REPORT DOCUMENTATION PAGE

*Form Approved
OMB No. 0704-0188*

Public reporting burden for this collection of information is estimated to average 1 hour per response, including the time for reviewing instructions, searching existing data sources, gathering and maintaining the data needed, and completing and reviewing the collection of information. Send comments regarding this burden estimate or any other aspect of this collection of information, including suggestions for reducing this burden, to Washington Headquarters Services, Directorate for Information Operations and Reports, 1215 Jefferson Davis Highway, Suite 1204, Arlington, VA 22202-4302, and to the Office of Management and Budget, Paperwork Reduction Project (0704-0188), Washington, DC 20503.

1. AGENCY USE ONLY (Leave blank)			2. REPORT DATE May 1992		3. REPORT TYPE AND DATES COVERED Technical Memorandum		
4. TITLE AND SUBTITLE Analysis and Modification of a Single-Mesh Gear Fatigue Rig for Use in Diagnostic Studies			5. FUNDING NUMBERS WU-505-63-36 1L162211A47A ✓				
6. AUTHOR(S) James J. Zakrajsek, Dennis P. Townsend, Fred B. Oswald, and Harry J. Decker							
7. PERFORMING ORGANIZATION NAME(S) AND ADDRESS(ES) NASA Lewis Research Center Cleveland, Ohio 44135-3191 and Propulsion Directorate U.S. Army Aviation Systems Command Cleveland, Ohio 44135-3191			8. PERFORMING ORGANIZATION REPORT NUMBER E-6826				
9. SPONSORING/MONITORING AGENCY NAMES(S) AND ADDRESS(ES) National Aeronautics and Space Administration Washington, D.C. 20546-0001 and U.S. Army Aviation Systems Command St. Louis, Mo. 63120-1798			10. SPONSORING/MONITORING AGENCY REPORT NUMBER NASA TM-105416 AVSCOM-TR-91-C-049				
11. SUPPLEMENTARY NOTES James J. Zakrajsek, Dennis P. Townsend, and Fred B. Oswald, NASA Lewis Research Center; Harry J. Decker, Propulsion Directorate, U.S. Army Aviation Systems Command. Responsible person, James J. Zakrajsek, (216) 433-3968.							
12a. DISTRIBUTION/AVAILABILITY STATEMENT Unclassified - Unlimited Subject Category 37			12b. DISTRIBUTION CODE				
13. ABSTRACT (Maximum 200 words) A single-mesh gear fatigue rig was analyzed and modified for use in gear mesh diagnostic research. The fatigue rig allowed unwanted vibration to mask the test-gear vibration signal, making it difficult to perform diagnostic studies. Several possible sources and factors contributing to the unwanted components of the vibration signal were investigated. Sensor mounting location was found to have a major effect on the content of the vibration signal. In the presence of unwanted vibration sources, modal amplification made unwanted components strong. A sensor location was found that provided a flatter frequency response. This resulted in a more useful vibration signal. A major rework was performed on the fatigue rig to reduce the influence of the most probable sources of the noise in the vibration signal. The slave gears were machined to reduce weight and increase tooth loading. The housing and the shafts were modified to reduce imbalance, looseness, and misalignment in the rotating components. These changes resulted in an improved vibration signal, with the test-gear mesh frequency now the dominant component in the signal. Also, with the unwanted sources eliminated, the sensor mounting location giving the most robust representation of the test-gear meshing energy was found to be at a point close to the test gears in the load zone of the bearings.							
14. SUBJECT TERMS Gears; Fatigue; Diagnostics			15. NUMBER OF PAGES 20		16. PRICE CODE A03		
17. SECURITY CLASSIFICATION OF REPORT Unclassified		18. SECURITY CLASSIFICATION OF THIS PAGE Unclassified		19. SECURITY CLASSIFICATION OF ABSTRACT Unclassified		20. LIMITATION OF ABSTRACT	